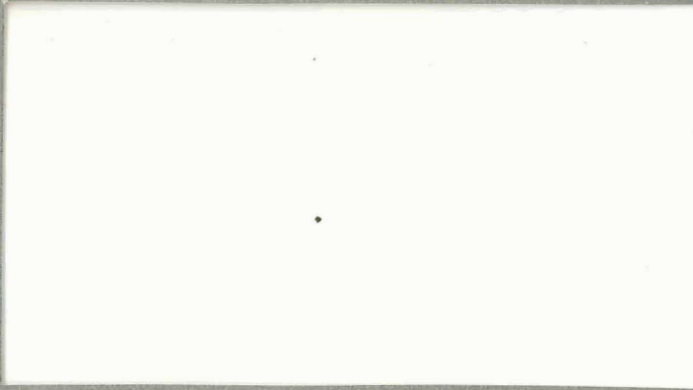
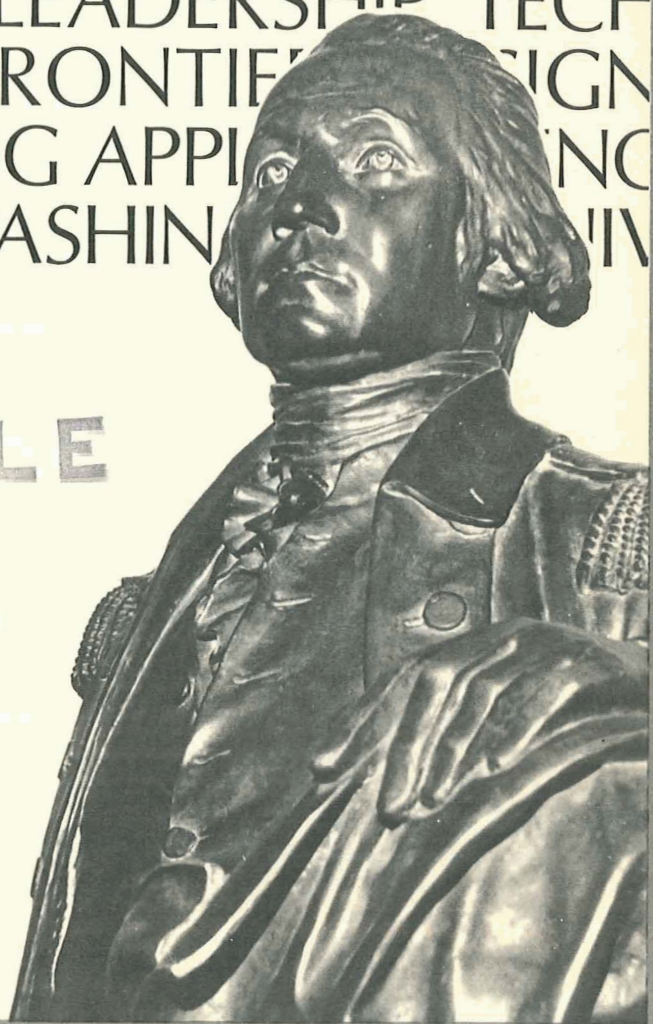


N 70 34400
NASA CR 66974



THE
GEORGE
WASHINGTON
UNIVERSITY

STUDENTS FACULTY STUDY R
ESEARCH DEVELOPMENT FUT
URE CAREER CREATIVITY CO
MMUNITY LEADERSHIP TECH
NOLOGY FRONTIER DESIGN
ENGINEERING APPLIED SCIENCE
GEORGE WASHINGTON UNIV



CASE FILE
COPY

SCHOOL OF ENGINEERING
AND APPLIED SCIENCE

INVARIANT IMBEDDING TECHNIQUE
APPLIED TO THE PROPAGATION OF
ELECTROMAGNETIC WAVES THROUGH
INHOMOGENEOUS RE-ENTRY PLASMAS

by

Terence Glenn Ryan

and

Robert B. Heller

June 7, 1970

Acknowledgement for support is given to the
National Aeronautics and Space Administration
(NASA Grant NGR-09-010-053)

School of Engineering and Applied Science
The George Washington University
Washington, D.C. 20006

PREFACE

The problem of communicating through a re-entry plasma arose out of a study being done by the George Washington University School of Engineering and Applied Science under the direction of Professor R. B. Heller for the National Aeronautics and Space Administration, Langley, Virginia. Propagation through re-entry plasmas, the topic of this study, is intended to serve as a contribution toward this effort. Lengthy computerized computational procedures have been utilized in the past to solve the inhomogeneous second order wave equation and thus predict propagation losses in an inhomogeneous media. This study presents a technique yielding approximate solutions that may be calculated without the use of a computer or lengthy computational procedures. Accuracies to within a few percent of those due to lengthy computer runs are obtained.

The re-entry communications problem is a serious one resulting in complete communication blackout during critical phases of space missions. It is the purpose of this study to develop, via an invariant imbedding technique, a means of predicting signal losses through an inhomogeneous re-entry plasma.

LIST OF FIGURES

<u>Figure</u>		<u>Page</u>
1	Problem Configuration	3
2	Typical Re-Entry Plasma Characteristics	9
3	Typical Re-Entry Profiles	10
4	Space Vehicle Re-Entry Profiles	11
5	Electron Density and Collision Frequency	12
6	Plasma Frequency and Collision Frequency at Re-Entry Vehicle Nose	13
7	Boundary Between Two Homogeneous Plasmas	18
8	Infinitesimal Slab Imbedded in Plasma	23
9	Reflection Components from Slab	24
10	Transmission Components From Slab	29
11	Index of Refraction as a Function of ω/ω_p and ν/ω_p	34
12	Absorption Coefficient as a Function of ω/ω_p and ν/ω_p	35
13	Plasma Propagation Loss Versus Frequency	38
14	Plasma Propagation Loss Versus Altitude	39
15	Comparison of Measured and Predicted Blackout Points for Apollo Re-Entry at S- Band	40

TABLE OF CONTENTS

	<u>Page</u>
Preface	i
List of Figures	ii
I. Introduction	1
II. Physical Processes During Re-Entry	2
III. Plasmas and their Descriptive Parameters	5
IV. Re-Entry Plasma	8
V. Computation Procedure	15
VI. Transmission Losses Through the Re-Entry Plasma	31
VII. Summary	41
VIII. Bibliography	42

I. Introduction

This study treats the problem of predicting electromagnetic propagation losses encountered between a spacecraft and ground station during spacecraft re-entry conditions. The problem has been shown to be a serious one resulting, for many cases, in a complete communications "blackout" between spacecraft and ground.

As a spacecraft enters the earth's atmosphere at orbital or greater velocities its kinetic energy begins to be dissipated in the form of heat due to friction with the surrounding atmosphere. At a certain point during re-entry, as the spacecraft nosecone and adjacent gases greatly increase in temperature, partial ionization of the surrounding atmospheric gases takes place. In this manner, a plasma is formed comprised of the positive and negative ions extending rearward and outward from the spacecraft nosecone. The plasma is always inhomogeneous in nature and its physical extent and electrical parameters are functions of the vehicle shape and trajectory. It is the goal of this study to determine the propagation characteristics (specifically, transmission loss) of electromagnetic energy through this inhomogeneous plasma engulfing the re-entering spacecraft.

The task has been broken down into two main problem areas. First, the physical and electrical characteristics of the re-entry plasma were established and second, a computational procedure was developed to calculate the propagation characteristics. The re-entry plasma characteristics were determined by performing an extensive literature survey covering both theoretical and measurement techniques used to describe the nature of the plasma. The propagation computations were carried out by applying the principles of the invariant imbedding procedure to the solution of the wave equation in an inhomogeneous plasma. Lastly, the Riccati type differential equation resulting from the invariant embedding approach was solved, using certain approximations, to yield values of reflection from and transmission through the inhomogeneous plasma region formed about a re-entering spacecraft.

II. Physical Processes During Re-Entry

As a missile or spacecraft re-enters the earth's atmosphere at orbital or greater velocities a plasma sheath is formed on its surface, degrading normal electromagnetic communications. The plasma sheath is created as a consequence of the vehicle's kinetic energy being dissipated into the surrounding atmosphere in the form of heat. Usually, the plasma completely surrounds the re-entering vehicle and extends far back into its wake. The extent of the plasma sheath has been found to be very much dependent on the vehicle size, shape, and entering velocity. Figure 1 depicts a vehicle re-entering the earth's atmosphere along with its accompanying plasma sheath. The following description provides a detailed account of the plasma formation process.

At the beginning of the re-entry sequence, the pressure in front of a vehicle builds up to more than a thousand times its normal value (several thousand psi), at the same time the surrounding gas temperature increases by tens of thousands of degrees in a time span of about 20 microseconds. This process is so severe and rapid that some of the chemical components of the surrounding atmosphere, particularly NO (Nitric Oxide), overshoot equilibrium conditions and become ionized. That is, electrons become excited and are stripped from their parent atoms. Thus, a hot ionized gas composed of positive and negative charges, or plasma, is formed near the front of the re-entering vehicle. The plasma then flows back along the body of the vehicle in a few tenths of a millisecond, expanding as it progresses, completely surrounding the vehicle. It is known that for blunt nose vehicles the plasma is formed mainly in the region of the nose. For the case of a thinner or sharper nosed vehicle the plasma is formed for the most part by frictional heating occurring along the sides of the vehicle.

The problem of accurately predicting the composition of a re-entry plasma is quite difficult if not beyond the state of art in many instances (particularly during planetary re-entry conditions). This problem is greatly

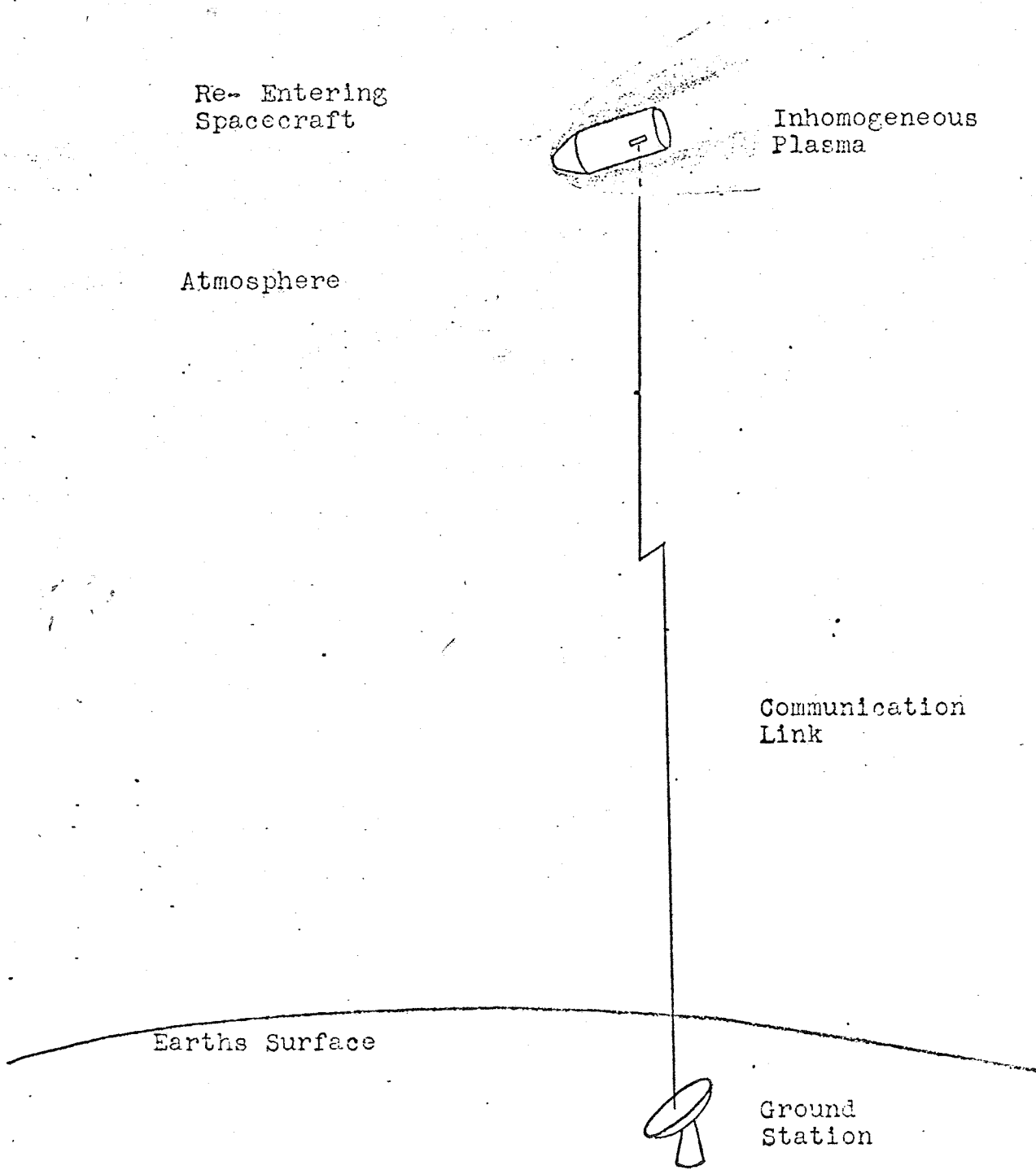


Figure I. PROBLEM CONFIGURATION

complicated due to the production and re-combining of ions from many different gases present in the plasma. The effects of thermodynamics, aerodynamics, and hot particles stripped from the vehicle nosecone by ablations must be considered simultaneously to obtain an accurate representation of the plasma composition.

Despite all these difficulties, accurate estimates of plasma properties have been made for several practical situations. A summary of typical re-entry plasma characteristics gathered from several different sources is presented later in this study.

III. Plasmas and Their Descriptive Parameters

Before proceeding further, a closer examination will now be made of what has been termed a "plasma." Plasmas will be categorized in this section in terms of "warm," "cold," "isotropic," and "non-isotropic." In addition, the quantities most commonly used to mathematically describe plasmas will be presented and discussed. A brief introduction to a plasma and its descriptive parameters will be given. A certain degree of knowledge concerning plasmas and their mathematical descriptors is necessary in order to fully understand this study.

A plasma may be defined as a collection of positively and negatively charged particles free to move about, and approximately equal in number. Thus, an ionized gas, previously shown in this study to be created during spacecraft re-entry, can be classified as a plasma according to the definition just stated. It should be noted that both types of charged particles need not be capable of movement in order to satisfy the plasma definition. This occurs for the case of ionized gas where it often happens that a rapidly varying electric field can easily move free electrons but has very little effect against the inertia of the much heavier ions. The plasma may also contain neutral particles.

The two quantities most commonly used to analytically describe properties of the type of plasma encountered in this study are the collision frequency ν , and the electron density, N_e . Other useful descriptive quantities that can be derived from the collision frequency and the electron density are the plasma frequency, ω_p , cyclotron frequency, ω_c , and the Debye length, λ_d . Each of these quantities is defined in the following list:

Collision Frequency. The mean free path length of an electron, λ , is the average distance traveled between collisions. The collision frequency of the electron is defined as the ratio of the speed of the electron, u , to its mean free path length. Therefore,

$$\nu \text{ (collision frequency)} = \frac{u \text{ (speed)}}{\lambda \text{ (mean path)}} \quad (3-1)$$

Electron Density. The electron density, N_e , can be defined simply as the number of free electrons present per unit volume.

Plasma Frequency. The plasma frequency, ω_p , is a quantity that is commonly used to describe or classify a plasma. It is defined by the relation:

$$\omega_p = \sqrt{\frac{N_e e^2}{m \epsilon_0}} \quad (3-2)$$

where N_e = electron density

e = electron charge

m = electron mass

ϵ = free space permittivity

Cyclotron Frequency. Another quantity sometimes used is the cyclotron frequency defined by the relation:

$$\omega_B = \frac{eB_0}{m} \quad (3-3)$$

where B_0 = magnetic field present

Debye Length. The Debye length, l_d , for a given plasma represents the transition dimension between macroscopic and microscopic effects. This means that the Debye length must be very small in comparison with the physical dimensions of the plasma in order for plasma characteristics, as used in this study, to be valid. The Debye length can be expressed by the relation:

$$\text{Debye length } (l_d) = \sqrt{\frac{\epsilon_0 KT}{N_e e^2}} \quad (3-4)$$

where K = Boltzmann's Constant

T = plasma temperature ($^{\circ}$ K)

A "warm" plasma, sometimes referred to as a compressible plasma is realized when the wavelength of an electromagnetic wave under consideration is less than the Debye length. In this type of plasma, propagation arising from the longitudinal compression and expansion of electrons may be present in addition to the more familiar transverse modes.

In a "cold" plasma the electromagnetic wavelength is greater than the Debye length. Only transverse modes of propagation are possible for this type of plasma.

Anisotropic plasmas exhibit the usual characteristic where the permittivity must be expressed as a tensor. The anisotropic behavior occurring in plasmas comes about as a consequence of the application of an external magnetic field. In this study the earth's magnetic field tends to make re-entry plasmas an anisotropic media. This effect will be shown to be small in most practical cases, namely it is nearly isotropic for short distance effects.

IV Re-Entry Plasmas

Figure 2 illustrates the relationships between several of the plasma properties just described for a re-entry plasma sheath. The lines labeled l_D are the loci of constant Debye length. The plasma frequency and electron density are plotted along the vertical axis and the temperature and electron velocity are shown along the horizontal axis. The B labeled lines represent the minimum magnetic field strength that must be present to significantly influence the re-entry plasma characteristics, making it manifest anisotropic effects.

Re-entry plasmas can be seen, from the relations of Figure 2, to typically exhibit "cold" characteristics since commonly used communication wavelengths are much greater than the possible Debye lengths for the re-entry plasma. In addition, it can be deduced from Figure 2 that a typical plasma will exhibit isotropic characteristics. This is true since the earth's magnetic field, less than a few tenths of a gauss, is much less than the values indicated by the minimum required B field lines. Hence, a re-entry plasma will, in many cases, appear cold and isotropic.

Spacecraft or missile re-entry velocity versus altitude profiles are shown in Figures 3 and 4. The figures show relationships for orbital, lunar, and interplanetary missions. The sources of the profile information are given in the figures.

Figure 5 shows electron density, N_e , and collision frequency, ν , as a function of re-entering spacecraft altitude and velocity. The plasma frequency and collision frequency can be found as a function of altitude, and various missions, from the relations of Figure 6.

The plasma properties at any point during the vehicle re-entry procedure can be found from Figures 3 through 6. First, re-entry altitude and velocity values can be found for any desired position during re-entry from Figures 3 and 4. Next, actual plasma parameters can be found by applying the altitude and velocity just obtained from Figures 3 and 4 to

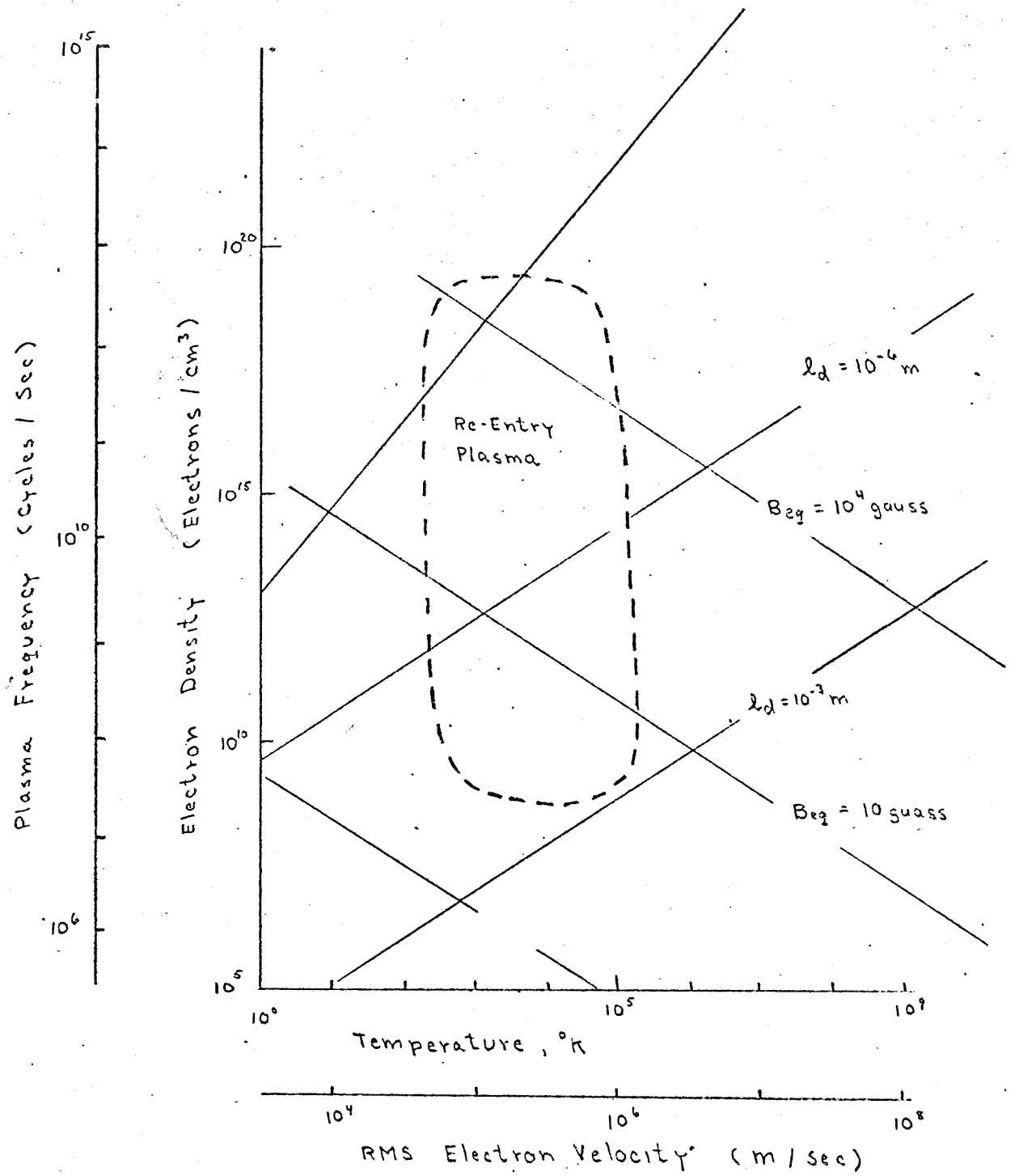


Figure 2. TYPICAL RE-ENTRY PLASMA CHARACTERISTICS [II]

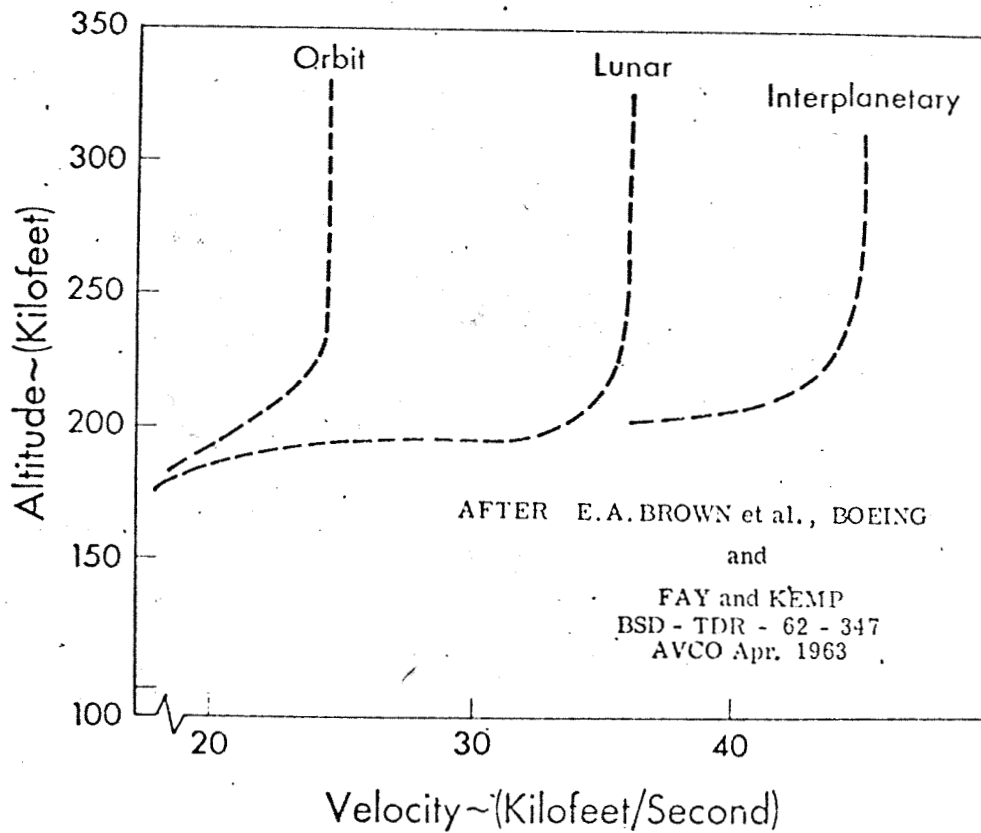


Figure 3. TYPICAL RE- ENTRY PROFILES

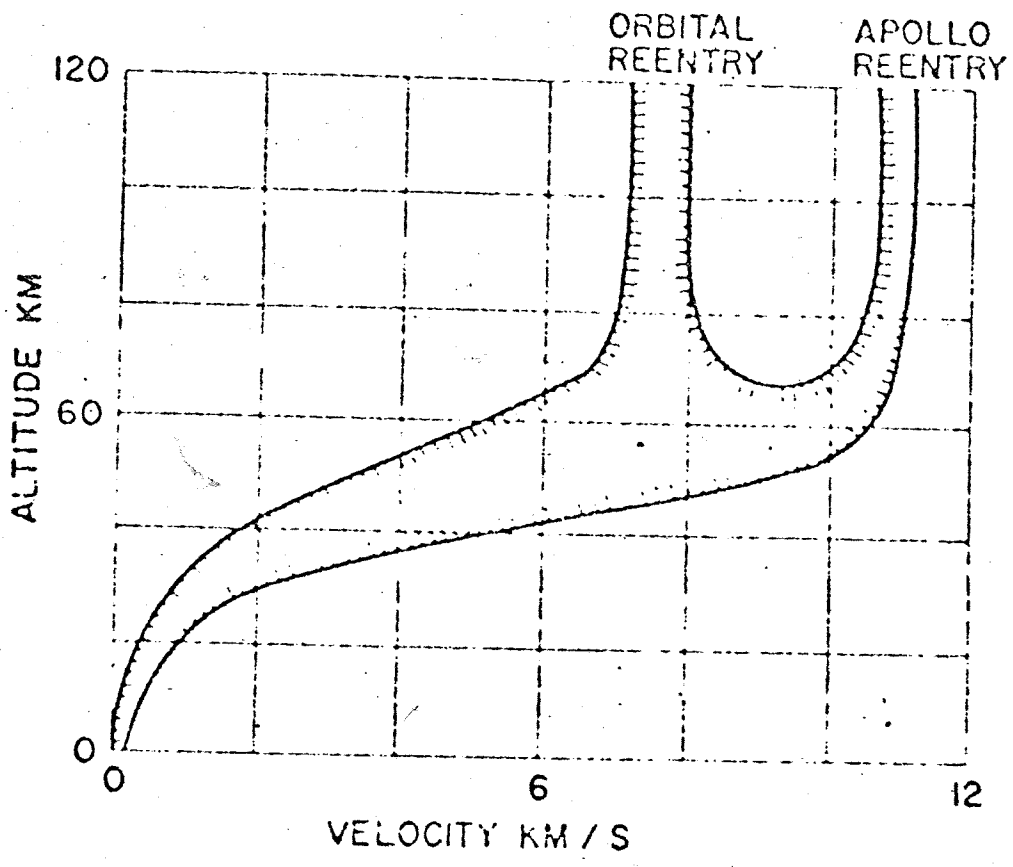


Figure 4. SPACE VEHICLE RE-ENTRY PROFILES [12]

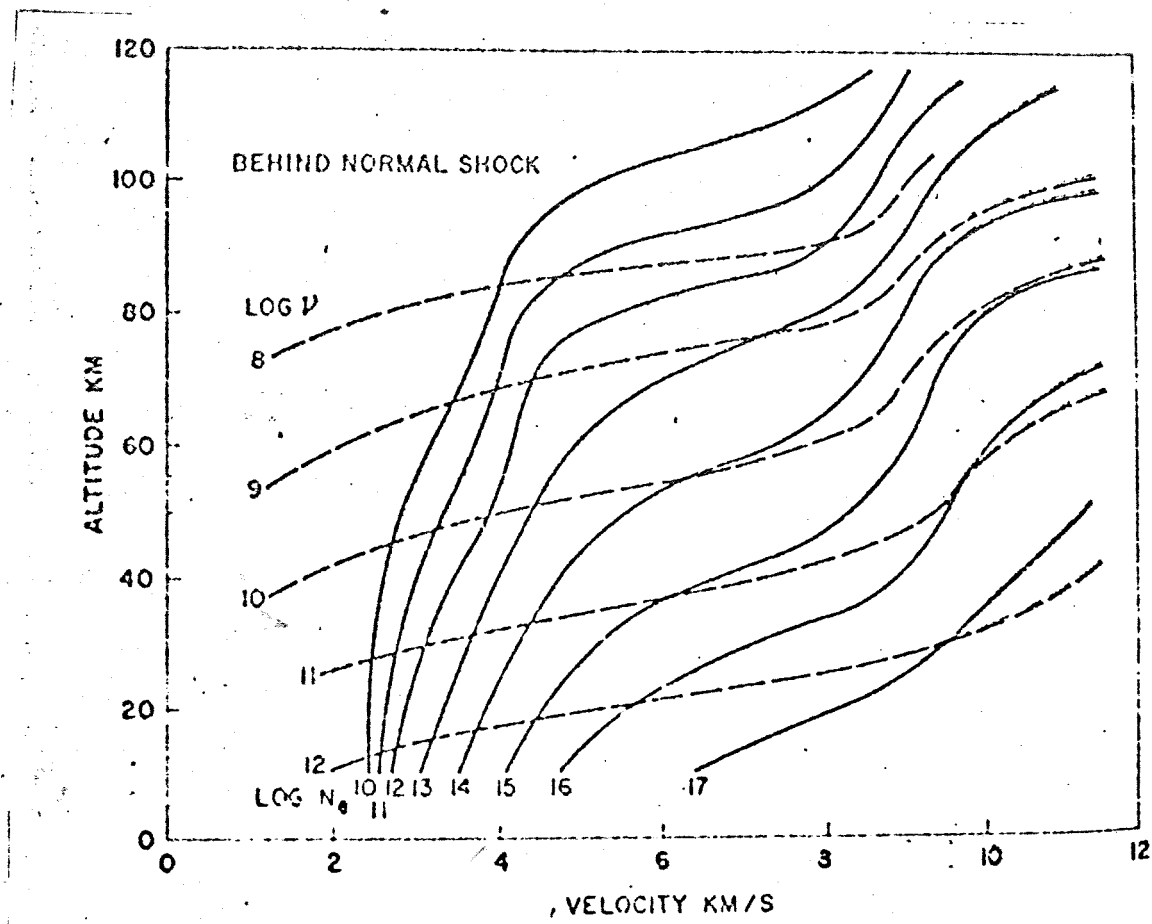
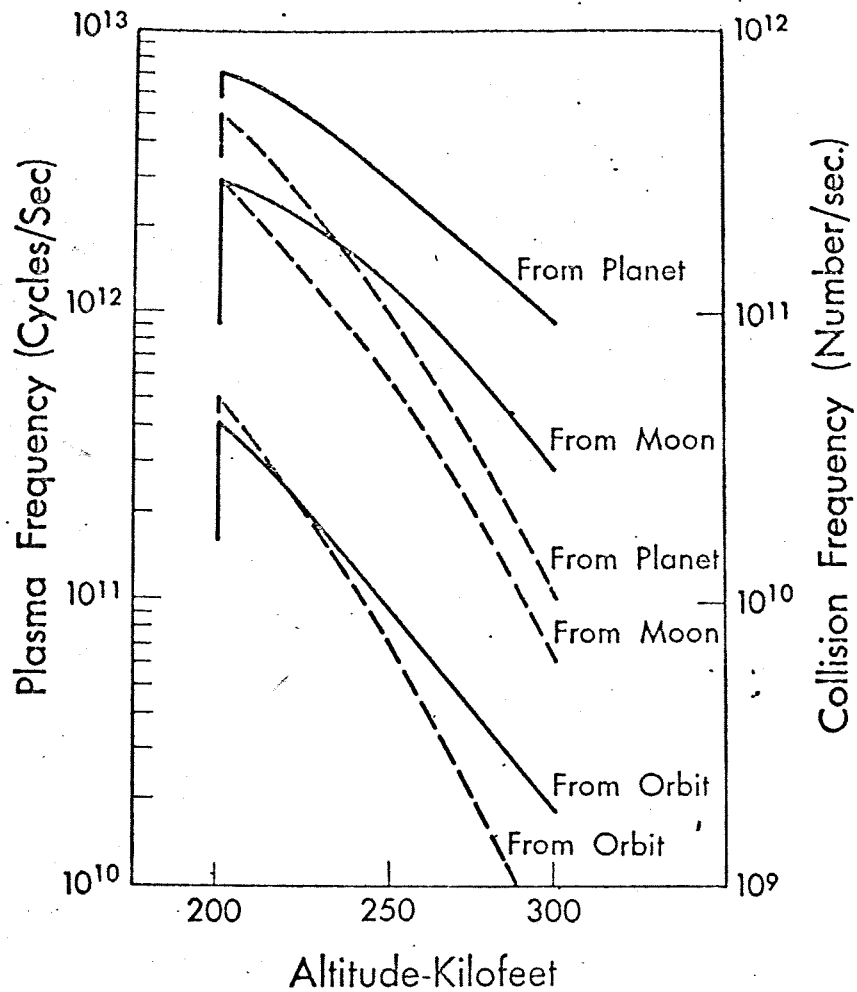


Figure 5. ELECTRON DENSITY AND COLLISION FREQUENCY [13]



Divide plasma frequency by 10 and collision frequency by 100 to obtain values along the spacecraft sides.

Figure 6. PLASMA FREQUENCY AND COLLISION FREQUENCY AT RE-ENTRY VEHICLE NOSE [3]

the relations of Figures 5 and 6. In this way numerical estimates of re-entry plasma parameters can be obtained at any point for various types of spacecraft missions.

V. Computation Procedure

The invariant imbedding computational procedure used in this study to calculate transmission losses through an inhomogeneous plasma begins with fundamental wave propagation properties. First, the reflection and transmission properties of an electromagnetic wave at a single boundary will be determined. Next, applying the principle of localization, the problem just solved will be imbedded in a nonhomogeneous medium (re-entry plasma) where the relation between two such surfaces separated by a very small distance (Δz) is determined. Finally, the limit is taken as the distance between the two adjacent problems approaches zero. A Riccati type differential equation is generated that describes the electromagnetic propagation through a inhomogeneous plasma.

Wave Propagation. The well known wave equation describing plane waves in free space can be expressed as:

$$\nabla^2 \bar{E} + k^2 \bar{E} = 0 \quad (5-1)$$

where \bar{E} = electric field vector

k = propagation constant

The solutions for this type of wave equation are of the form

$$\bar{E} = \bar{E}_0 e^{j(\omega t + kz)}$$

where $\omega = 2\pi f$

t = time

(5-2)

\bar{E}_0 = a constant vector

z is in the direction of propagation and the minus sign denotes a forward traveling wave and the plus sign a backward traveling wave. For a nonhomogeneous media the same basic form of the wave equation applies except that $k = k(z)$ and the solution can no longer be simply determined as in the homogeneous media case. The propagation constant k is no longer constant (varying with z) and will henceforth be referred to as the propagation factor.

Typical re-entry plasmas were shown previously to be isotropic but nonhomogeneous in nature. Relations describing the propagation factors for "cold" and "warm" plasma regions are presented below:

cold plasma

$$k = \omega \sqrt{\mu_0 \epsilon_0} [n + j\alpha] \quad (5-3)$$

where α , the absorption coefficient is

$$\alpha = \text{Im} \left[1 - \frac{(\omega_p/\omega)^2}{1 - j\nu/\omega} \right]^{\frac{1}{2}} \quad (5-4)$$

and n , the index of refraction can be expressed as

$$n = \text{Re} \left[1 - \frac{(\omega_p/\omega)^2}{1 - j\nu/\omega} \right]^{\frac{1}{2}} \quad (5-5)$$

warm plasma

$$\alpha = \text{Im} \left[\frac{1 - \frac{(\omega_p/\omega)^2}{1 - j\nu/\omega}}{1 - \frac{(\omega_p/\omega)^2}{(1 - j\nu/\omega)^3} \frac{KT}{mc^2}} \right]^{\frac{1}{2}} \quad (5-6)$$

$$n = \text{Re} \left[\frac{1 - \frac{(\omega_p/\omega)^2}{1 - j\nu/\omega}}{1 - \frac{(\omega_p/\omega)^2}{(1 - j\nu/\omega)^3} \frac{KT}{mc^2}} \right]^{\frac{1}{2}} \quad (5-7)$$

where m = mass of electron

c = speed of light in a vacuum

K = Boltzman constant

T = Kelvin temperature

ν = collision frequency

Transmission and Reflection at a Single Boundary

The first step of the invariant imbedding process is to determine the reflection and transmission from a plane boundary separating two semi-infinite homogeneous plasmas as illustrated in Figure 7. The incident wave is assumed to a plane wave traveling in the z direction and an electric field component only in the x direction as shown in Figure 7.

At the boundary between the two plasmas, E and E' (i.e., $E' = \frac{\partial E}{\partial z}$) are continuous. This boundary condition can be derived from Maxwells Equations as follows:

$$\nabla \times \bar{E} = -\frac{\partial \bar{B}}{\partial t} \quad (5-8)$$

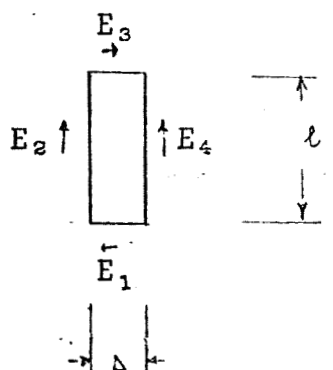
where \bar{B} = magnetic flux density

applying Stokes Theorem,

$$\oint (\nabla \times \bar{E}) \cdot d\bar{s} = \oint \bar{E} \cdot d\bar{l} \quad (5-9)$$

$$\therefore \oint \bar{E} \cdot d\bar{l} = -\oint \frac{\partial}{\partial t} \bar{B} \cdot d\bar{s} \quad (5-10)$$

taking the line integral around the rectangle shown in the figure below gives



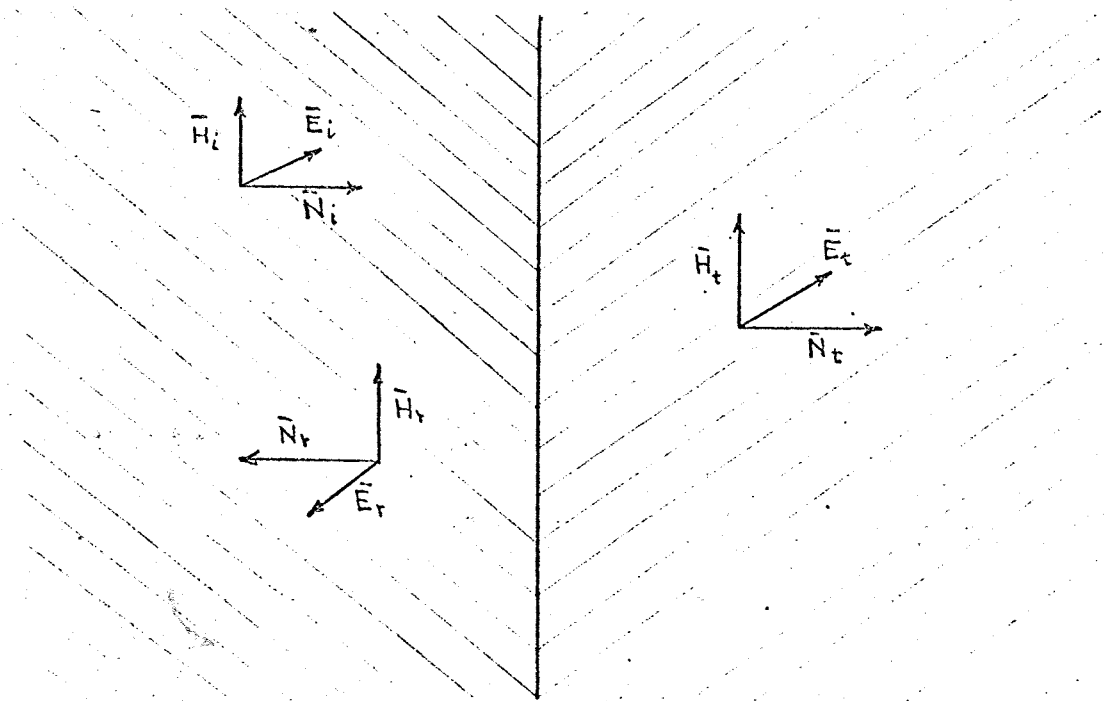
$$E_1 \Delta + E_2 l + E_3 \Delta - E_4 l = \oint \bar{E} \cdot d\bar{l} \quad (5-11)$$

$$(E_2 - E_4) l = \oint \bar{E} \cdot d\bar{l}$$

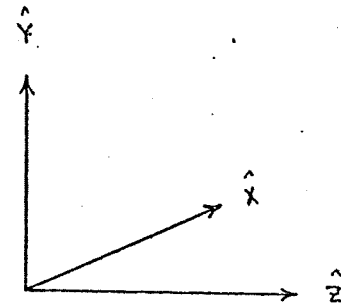
The area of the rectangle is zero since two sides are of length Δ and therefore the contribution from a finite time changing magnetic flux is zero.

Homogeneous Plasma 1

Homogeneous Plasma 2



i indicates incident
 t indicates transmitted
 r indicates reflected
 \vec{N} = Poynting Vector



Coordinates used for
 calculations

Figure 7. BOUNDARY BETWEEN TWO HOMOGENEOUS PLASMAS

Hence,

$$(E_2 - E_4) l = \oint \bar{E} \cdot d\bar{l} = - \oint \frac{\partial}{\partial t} \bar{B} \cdot d\bar{s} = 0 \quad (5-12)$$

$$(E_2 - E_4) l = 0 \quad (5-13)$$

or $E_2 = E_4$ (continuity of E)

The continuity of E' will now be established starting with Maxwells fourth equation,

$$\nabla \cdot \bar{H} = \bar{i} + \frac{\partial \bar{D}}{\partial t} \quad (5-14)$$

Continuity of H can be established from a process similar to that just used for E, so the proof will be omitted here. For a sinusoidal time variation Maxwells third equation

$$\nabla \times \bar{E} = - \frac{\partial \bar{B}}{\partial t} \quad (5-15)$$

can be changed to $\nabla \times \bar{E} = -j\omega\mu \bar{H}$

expanding $\nabla \times \bar{E}$ into its \hat{X} , \hat{Y} , and \hat{Z} components gives

$$\left(\frac{\partial E_z}{\partial y} - \frac{\partial E_y}{\partial z} \right) \hat{x} + \left(\frac{\partial E_x}{\partial z} - \frac{\partial E_z}{\partial x} \right) \hat{y} + \left(\frac{\partial E_y}{\partial x} - \frac{\partial E_x}{\partial y} \right) \hat{z} = -j\omega\mu \bar{H}$$

since $E_z = E_y = 0$, and variation is only in the z direction ($\frac{\partial}{\partial x} = \frac{\partial}{\partial y} = 0$)

this equation reduces to

$$\frac{\partial E_x}{\partial z} = -j\omega\mu H_y \quad (5-17)$$

or, $E' = C H$ $C = \text{a constant } (-j\omega\mu)$

Thus E' must be continuous at the boundary since continuity of H has been previously assumed to be developed.

Due to continuity of E at the boundary, the sum of the incident and reflected waves must equal the transmitted wave,

$$E_i e^{j(\omega t - k_1 z)} + E_r e^{j(\omega t + k_1 z)} = E_t e^{j(\omega t - k_2 z)} \quad (\text{at boundary}) \quad (5-18)$$

omitting the common factor $e^{j\omega t}$ for simplicity

$$E_i e^{-jk_1 z} + E_r e^{jk_1 z} = E_t e^{-jk_2 z} \quad (5-19)$$

letting the boundary be at $Z = 0$

$$E_i + E_r = E_t. \quad (5-20)$$

Differentiating equation 5-19 with respect to z yields

$$-jk_1 E_i e^{-jk_1 z} + jk_1 E_r e^{jk_1 z} = -jk_2 E_t e^{-jk_2 z} \quad (5-21)$$

at $Z = 0$ this becomes

$$-jk_1 E_i + jk_1 E_r = -jk_2 E_t. \quad (5-22)$$

Multiplying equation 5-20 by k_1 ; equation 5-22 by -1 , and adding with equation 5-22 gives

$$k_1 E_i + k_1 E_r = k_1 E_t \quad (5-23)$$

$$k_1 E_i - k_1 E_r = k_2 E_t$$

$$\hline 2k_1 E_i = k_1 E_t + k_2 E_t$$

thus, the ratio of the transmitted wave to the incident wave is

$$\frac{E_t}{E_i} = \frac{2k_1}{k_1 + k_2}. \quad (5-24)$$

The reflected portion of the wave can be found by dividing equation 5-20 by E_i and using the results of equation 5-24.

$$1 + \frac{E_r}{E_i} = \frac{E_t}{E_i} \quad (\text{dividing 5-20 by } E_i)$$

$$1 + \frac{E_r}{E_i} = \frac{2 k_1}{k_1 + k_2} \quad (\text{using 5-24})$$

From 5-24 the reflected wave is found to be

$$\frac{E_r}{E_i} = \frac{k_1 - k_2}{k_1 + k_2} \quad (5-25)$$

At this point, both the reflected and transmitted portion of a wave resulting from the discontinuity between two semi-infinite homogeneous plasma regions has been established.

Principle of Localization

The principle of localization states that "a plane wave traveling through an inhomogeneous medium proceeds as if there were an instantaneous reflection and transmission at each interface of a stratum $[z, z + \Delta z]$. These reflections and transmissions occur as if the stratum were actually a semi-infinite homogeneous medium with propagation constant $k(z)$ at all points beyond z ." This principle allows one to "imbed" the problem just solved into an inhomogeneous media since at each point the media acts as if it were constructed of two semi-infinite homogeneous plasmas.

The problem just solved may be considered as a particular process that is a member of a family of similar processes. When the particular process is imbedded in an inhomogeneous media the functional relations connecting different members of the family of similar processes may be determined. In this way an insight is gained into the process that is quite different than that obtained by consideration of the isolated

process (i.e., reflection at a single boundary).

The next step in the invariant imbedding process involves determining the relation between two adjacent problems and expanding this to describe propagation throughout the entire medium.

Invariant Imbedding

The reflection and transmission coefficients previously developed for one surface discontinuity will now be applied to determine the reflection from two such discontinuities.

A very small section of width Δz of the inhomogeneous media is depicted in Figure 8. To the left of z the propagation factor is considered to be a constant k . Inside the Δz width the propagation factor has a constant value denoted by $k(z + \Delta z)$. Figure 9 depicts the various reflected wave components and their propagation directions. The incoming incident wave has been normalized to one in order to simplify the computations that follow. In order to include the effects of all the zeroth and first order terms in Δz , the reflections and transmissions shown in Figure 9 will be taken into account.

Figure 9a accounts for the reflected E wave from the boundary at z . Figure 9b accounts for transmission through z , reflection from $z + \Delta z$ and transmission back out through the boundary at z . In Figure 9c the wave passes through z , is reflected at $z + \Delta z$, travels back to z where it is reflected back to $z + \Delta z$ and is again reflected and finally travels out through z . Mathematically this procedure can be written as follows:

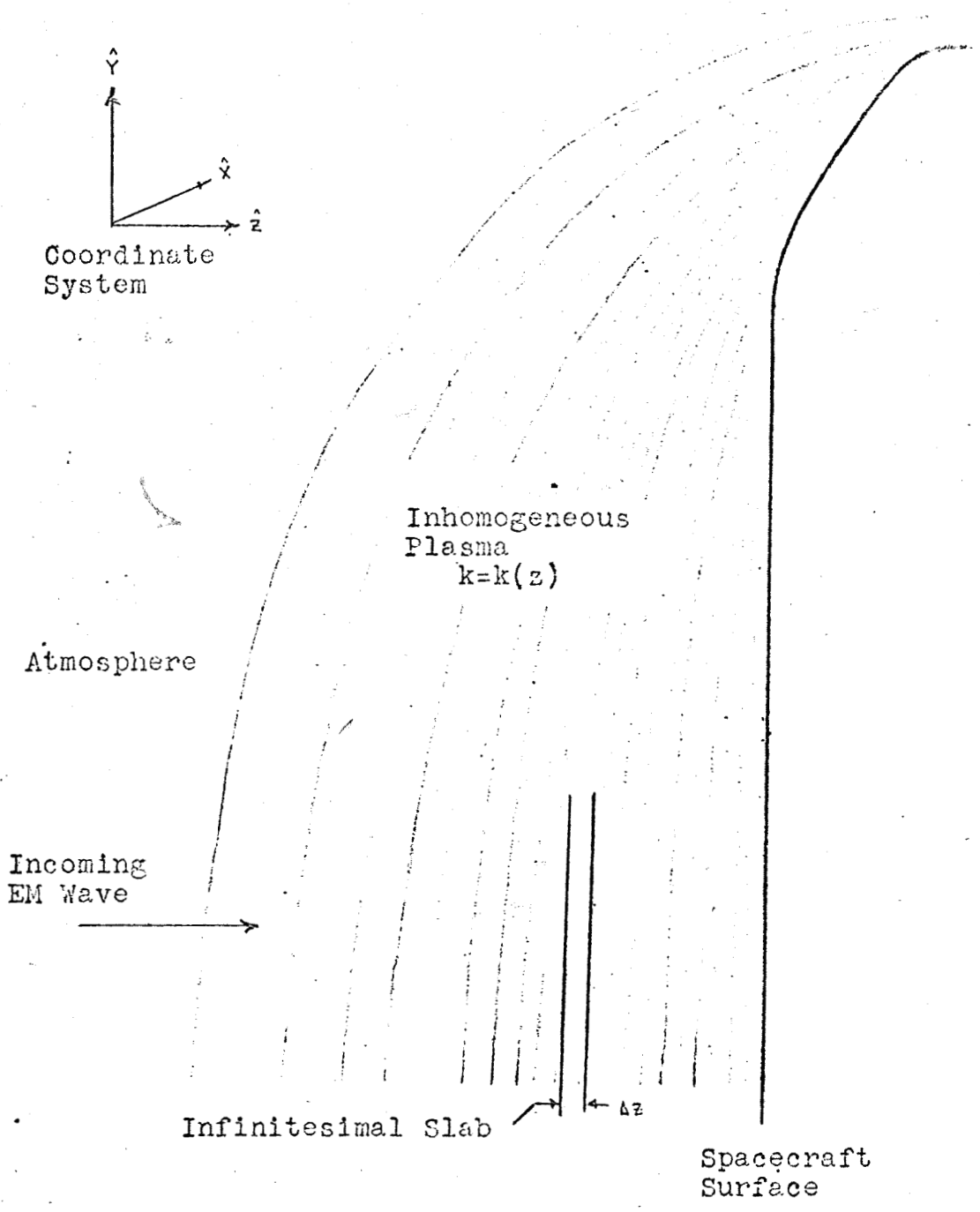


Figure 8. Infinitesimal Slab Imbedded In Plasma

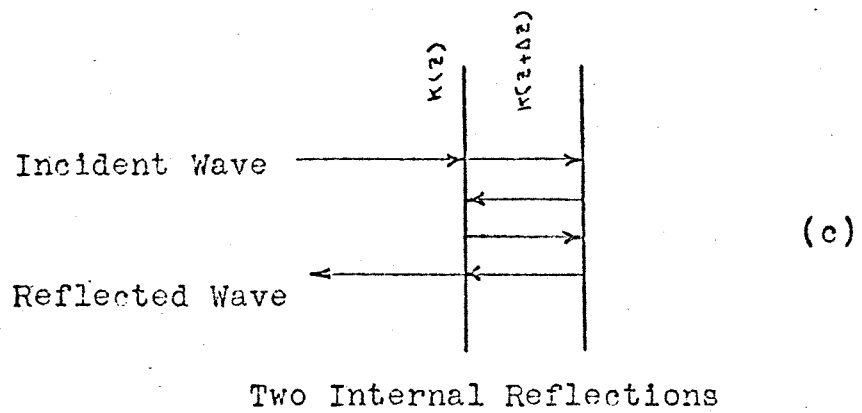
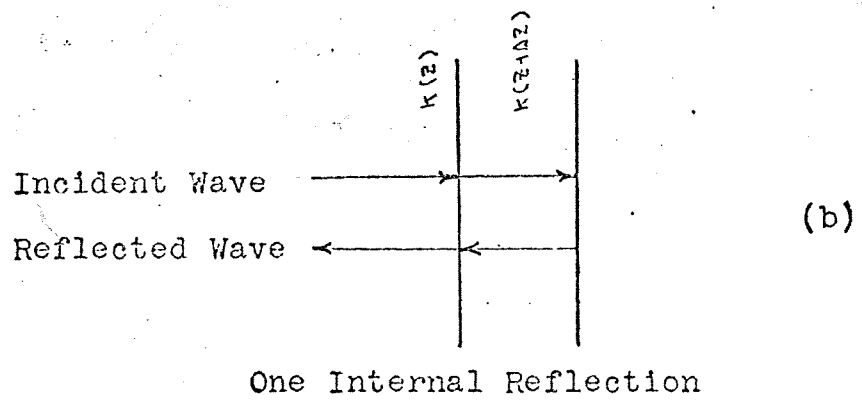
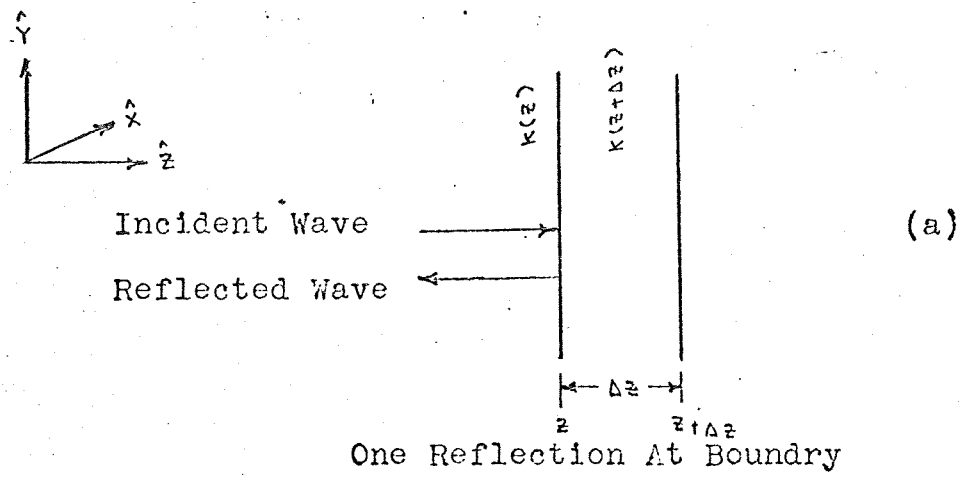


Figure 9. REFLECTION COMPONENTS FROM SLAB

reflection from z

$$E_r(z) = \frac{k(z) - k(z+\Delta z)}{k(z) + k(z+\Delta z)} + \quad (\text{see Figure 9a})$$

transmission at z	travel to z + Δz	wave at z + Δz	travel back to z
$\frac{2k(z)}{k(z) + k(z+\Delta z)}$	$e^{-jk(z+\Delta z)\Delta z}$	$E_r(z+\Delta z)$	$e^{jk(z+\Delta z)(-\Delta z)}$

transmission out at z

$$\frac{2k(z+\Delta z)}{k(z) + k(z+\Delta z)} \quad (\text{see Figure 9b})$$

transmission at z	travel to z + Δz	wave at z + Δz	travel back to z
$\frac{2k(z)}{k(z) + k(z+\Delta z)}$	$e^{-jk(z+\Delta z)\Delta z}$	$E_r(z+\Delta z)$	$e^{jk(z+\Delta z)(-\Delta z)}$

reflection at z	travel to z + Δz	wave at z + Δz	travel back to z
$\frac{k(z+\Delta z) - k(z)}{k(z+\Delta z) + k(z)}$	$e^{-jk(z+\Delta z)\Delta z}$	$E_r(z+\Delta z)$	$e^{jk(z+\Delta z)(-\Delta z)}$

transmission
through z

(5-26)

$$\frac{2k(z)}{k(z+\Delta z) + k(z)} \quad (\text{see Figure 9c})$$

multiplying both sides of this equation by $-\frac{[k(z)+k(z+\Delta z)]}{2k(z)\Delta z}$
 results in

$$-\frac{E_r(z)[k(z)+k(z+\Delta z)]}{2k(z)\Delta z} = \frac{k(z+\Delta z)-k(z)}{\Delta z} \cdot \frac{1}{2k(z)}$$

$$-E_r(z+\Delta z)e^{-2jk(z+\Delta z)\Delta z} \frac{2k(z+\Delta z)}{k(z)+k(z+\Delta z)} \cdot \frac{1}{\Delta z}$$

$$-E_r(z+\Delta z)e^{-j4k(z+\Delta z)\Delta z} \frac{k(z+\Delta z)-k(z)}{k(z+\Delta z)+k(z)} E_r(z+\Delta z)$$

$$\frac{2k(z)}{k(z+\Delta z)+k(z)} \cdot \frac{1}{\Delta z} \quad (5-27)$$

Rearranging, expanding $e^{-j2k(z+\Delta z)\Delta z}$ into $1-j2k(z+\Delta z)\Delta z$,
 and taking the limit as $\Delta z \rightarrow 0$ yields

$$\lim_{\Delta z \rightarrow 0} \left\{ \frac{E_r(z+\Delta z) \left[\frac{2k(z+\Delta z)}{k(z)+k(z+\Delta z)} \right] - E_r(z) \left[\frac{k(z)+k(z+\Delta z)}{2k(z)} \right]}{\Delta z} \right\} =$$

$$\frac{1}{2k} \lim_{\Delta z \rightarrow 0} \left[\frac{k(z+\Delta z)-k(z)}{\Delta z} \right] -$$

$$2jk \lim_{\Delta z \rightarrow 0} \left\{ \frac{E_r(z+\Delta z) k(z+\Delta z) 2k(z+\Delta z)}{k(z)+k(z+\Delta z)} \right\} -$$

$$\lim_{\Delta z \rightarrow 0} \left\{ \frac{k(z+\Delta z)-k(z)}{\Delta z} [E_r(z+\Delta z)]^2 \frac{2k(z)}{k(z+\Delta z)+k(z)} e^{-j4k(z+\Delta z)\Delta z} \right\}$$

(5-28)

The definition of a derivative can be expressed as

$$\frac{dy}{dx} = Y' = \lim_{\Delta x \rightarrow 0} \left\{ \frac{f(x + \Delta x) - f(x)}{\Delta x} \right\}$$

For the case of the reflected electric field this expression becomes

$$E_r' = \lim_{\Delta z \rightarrow 0} \left\{ \frac{E_r(z + \Delta z) - E_r(z)}{\Delta z} \right\} \quad (5-29)$$

By applying this definition to the various parts of equation (5-28) and taking all the limits, equation (5-28) converges to

$$E_r' = \frac{k'}{2k} - 2j k E_r - \frac{k'}{2k} E_r^2 \quad (5-30)$$

a Riccati type equation describing the resultant electric field to the left of the non-homogeneous plasma.

The transmitted wave can be found by a similar procedure. Figure 10 depicts the reflected and transmitted components that need to be considered to include all terms in the zeroth and first order in Δz . The first component of the transmitted wave passes through z and then $z + \Delta z$ as shown in Figure 10a. The second component illustrated by Figure 10b passes through z , is reflected at $z + \Delta z$ and again at z , and finally emerges through $z + \Delta z$.

This process can be described mathematically by the equation

transmitted at z	travel to $z + \Delta z$	transmitted wave at $z + \Delta z$	
$\frac{2k(z)}{k(z) + k(z + \Delta z)}$	$e^{-jk(z + \Delta z)\Delta z}$	$E_T(z + \Delta z)$	(see Figure 10a)

transmitted through z	travel to $z + \Delta z$	refl. wave at $z + \Delta z$	travel to z
$\frac{2k(z)}{k(z) + k(z + \Delta z)}$	$e^{-jk(z + \Delta z)\Delta z}$	$E_T(z + \Delta z)$	$e^{jk(z + \Delta z)(-\Delta z)}$

reflection at z	travel to $z + \Delta z$	transmitted wave at $z + \Delta z$	
$\frac{k(z + \Delta z) - k(z)}{k(z + \Delta z) + k(z)}$	$e^{-jk(z + \Delta z)\Delta z}$	$E_T(z + \Delta z)$	(see Figure 10b)

(5-31)

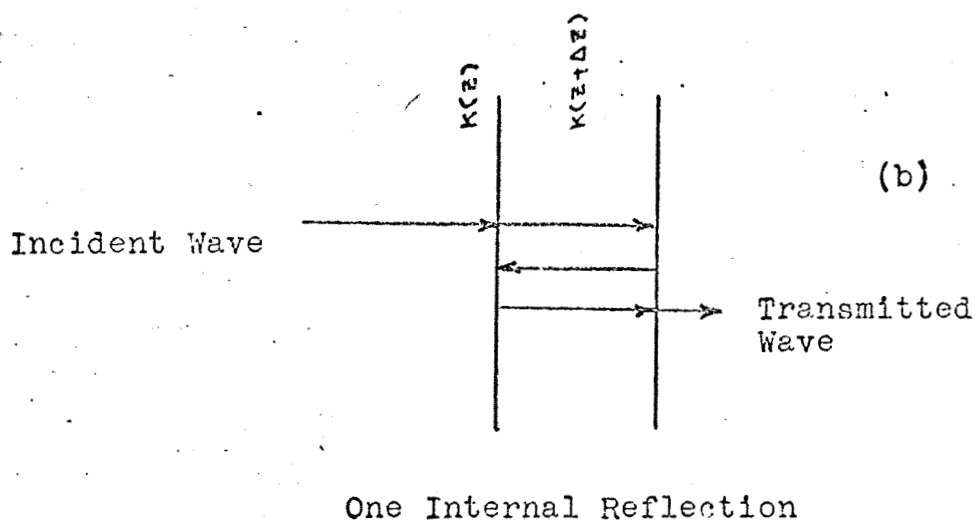
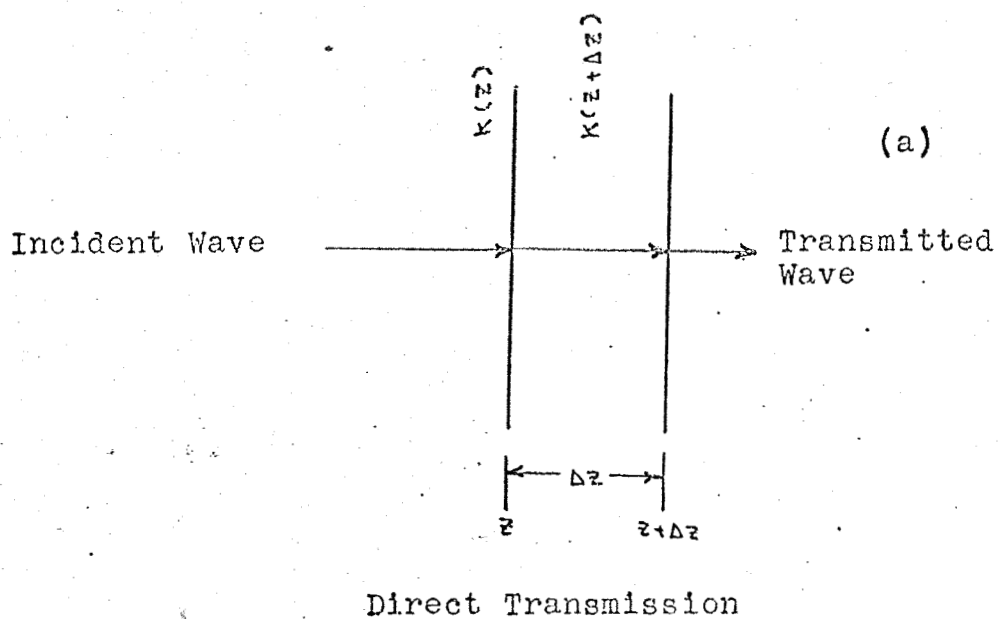


Figure 10. TRANSMISSION COMPONENTS FROM SLAB

Dividing this equation by Δz and taking the limit as $\Delta z \rightarrow 0$ using the same procedures as was done in the previous reflection case (equation 5-28) gives

$$E_r' = \left(\frac{k'}{2k} - E_r \frac{k'}{2k} - jk \right) E_r \quad (5-32)$$

where E_T now represents the transmitted wave.

Thus, a Riccati type differential equation representing the reflected wave

$$E_r' = \frac{k'}{2k} - 2jkE_r - \frac{k'}{2k} E_r^2 \quad (5-30)$$

and the corresponding equation for the transmitted wave

$$E_T' = \left(\frac{k'}{2k} - E_T \frac{k'}{2k} - jk \right) E_T \quad (5-32)$$

have been derived for an inhomogeneous plasma using the principles of invariant imbedding.

The type of differential equations just derived for the reflected and transmitted waves are solvable using computerized techniques, and are being done by Dr. R. Heller, of GWU. This avenue of solution will not be explored in this study but instead, certain approximate analytical solutions, already developed, will be employed in the next section to give numerical answers to the re-entry plasma propagation problem.

VI. Transmission Losses Through the Re-Entry Plasma

In the preceding section, differential equations were developed describing the reflection from and transmission through an inhomogeneous plasma. In this section these equations will be solved, under certain conditions, for propagation losses actually encountered during re-entry communication procedures. Two previously developed approximate solutions to the Riccati equation for the transmitted wave will be used to predict transmission losses through the plasma. The re-entry plasma characteristics will be taken from the information gathered in the first part of this study.

The approximate solutions [8] to the Riccati equation for the transmitted wave (eq. 5-32) mentioned above are called the Bremmer approximation and the MSG (Moberg, Schiff, Glauber) approximation. These approximations were generated by starting with an assumed solution to the Riccati differential equation and then performing successive iterations to obtain a more accurate solution. This procedure is quite lengthy and is completely developed in reference [8].¹ The following paragraph discusses the restrictions that must be placed on the re-entry plasma in order to make the approximate solutions valid.

If a plasma composition is approximated by the characteristic

$$N_e(z) = N_e \frac{z}{h} \quad (6-1)$$

where z = distance within plasma

h = plasma thickness

and by

$$\nu(z) = \nu = \text{constant} \quad (6-2)$$

the Bremmer and MSG approximations in the form expressed below, may be used to solve the transmission equation (equation 5-32). The first restriction

¹ The development appears on pp. 37-72 and the final results in the form used here are shown on pp. 89, 90.

on the plasma, $N_e = N_e \frac{z}{h}$ (eq. 6-1), simply means that the electron density varies linearly from a maximum value, N_e , at the space vehicle skin to zero at some distance h . $\nu(z) = \nu$ states that the collision frequency is assumed to have a constant value throughout the plasma.

Under the above conditions the Bremmer approximation can be expressed as

$$T_B = K^{\frac{1}{2}} \exp \left(j K_1 h \frac{2K^2 - K - 1}{3K + 3} \right) \quad (6-3)$$

where T_B = Bremmer transmission coefficient

K = relative propagation factor

$$K_1 = \omega \sqrt{\mu_0 \epsilon_0}$$

h = plasma thickness

and the MSG approximation may be written as

$$T_{MSG} = \frac{2}{1+K} \exp \left(j K_1 h \frac{K-1}{2} \right) \quad (6-4)$$

The accuracy of these two approximations [8] is shown in the table below.

Approximation	Relative Amplitude Error	Error-in Phase
MSG	zero	$(K_0^4 / 8K_1^4) K_1 h$
Bremmer	$K_0^4 / 12K_1^4$	zero

It can be seen that the MSG approximation is preferred where the amplitude errors are of chief concern and the Bremmer approximation is superior where phase errors are critical.

A sample calculation will now be made to illustrate the computational procedure.

First, an altitude - velocity point is determined from Figure 3 or Figure 4. Choosing an altitude of 250 Kilofeet from Figure 3 gives a velocity of approximately 24 thousand feet per second for an orbital re-entry vehicle. Using these values, the collision frequency, ν , and the electron density can be found from Figure 5. The propagation factor K can then be calculated from the previously presented equations

$$K = \omega \sqrt{\mu_0 \epsilon_0} [n + j\alpha] \quad (6-5)$$

where α , the absorption coefficient is

$$\alpha = \text{Im} \left[1 - \frac{(\omega_p/\omega)^2}{1 - j\nu/\omega} \right]^{\frac{1}{2}} \quad \omega_p = \sqrt{\frac{N_e e^2}{m \epsilon_0}} \quad (6-6), (6-7)$$

and n , the index of refraction is

$$n = \text{Re} \left[1 - \frac{(\omega_p/\omega)^2}{1 - j\nu/\omega} \right]^{\frac{1}{2}} \quad (6-8)$$

- where
- $\omega = 2\pi f$ rad/sec
 - ω_p = plasma frequency, cycles/sec
 - ν = collision frequency, collisions/sec
 - N_e = electron density, electrons/meter³
 - e = electron charge, coulombs
 - m = electron mass, kilograms
 - ϵ_0 = free space permittivity, farads/meter

Or the plasma frequency and collision frequency may be determined directly from the curves of Figure 6 where for 250 kilofeet altitude it can be seen that $\omega_p \approx 9 \times 10^9$ cycles/sec, and $\nu \approx 7 \times 10^7$ collisions/sec. The index of refraction and absorption coefficient can be found directly, without the use of equations 6-6, 6-7, and 6-8 by computing the ratios $\frac{\omega}{\omega_p}$, ν/ω_p , and using the relations of Figures 11 and 12 respectively. Assuming a frequency of 10 KMHz (x band)

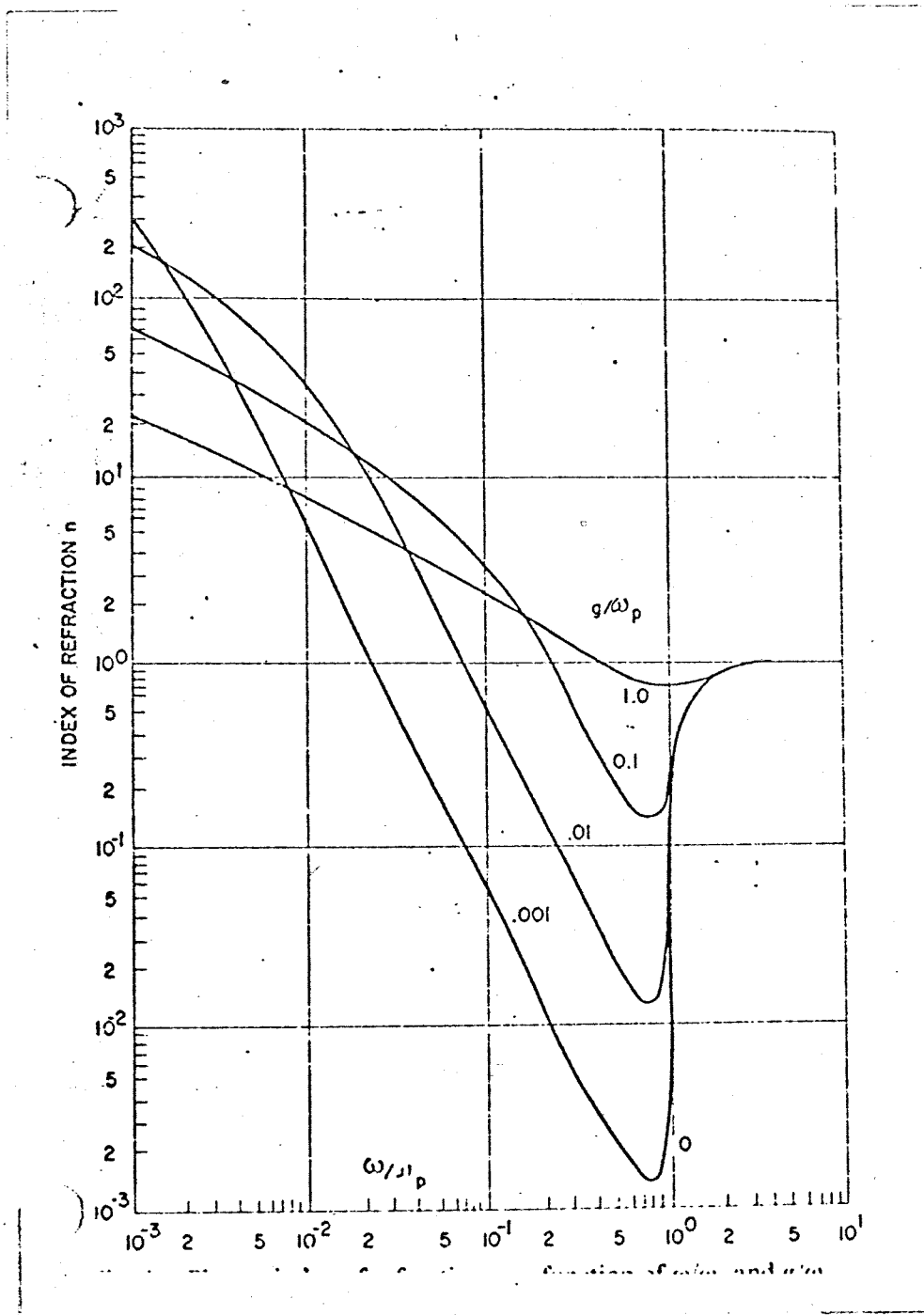


Figure 11. INDEX OF REFRACTION AS A FUNCTION OF ω/ω_p AND ν/ω_p . [14]

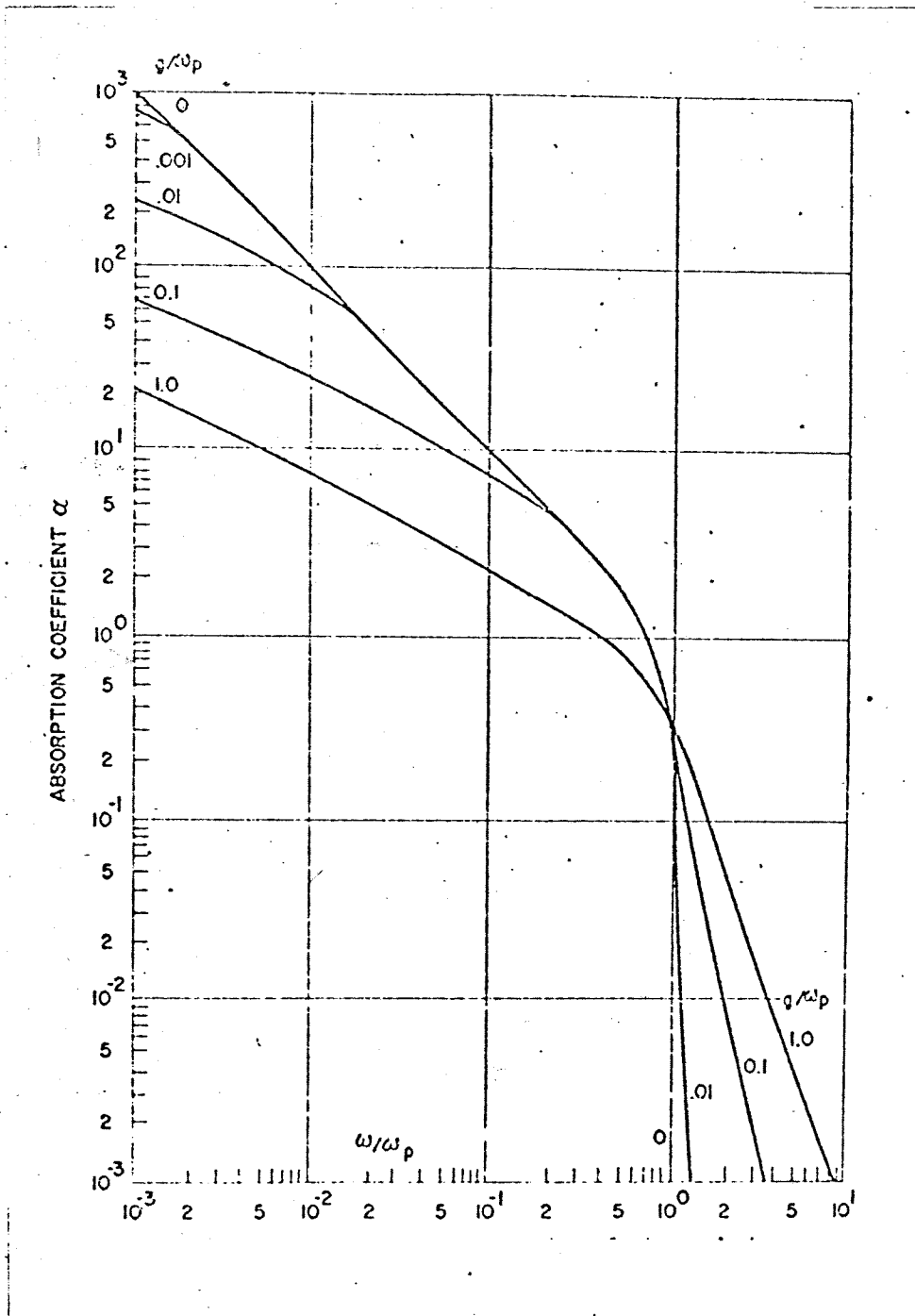


Figure 12. ABSORPTION COEFFICIENT AS A FUNCTION OF ω/ω_p AND ν/ω_p . [14]

$$\frac{\omega}{\omega_p} = \frac{10 \times 10^9}{9 \times 10^9} = 1.11 \quad (6-9)$$

$$\frac{\nu}{\omega_p} = \frac{7 \times 10^7}{2\pi \times 9 \times 10^9} = .00124 \quad (6-10)$$

from Figures 11 and 12

$$n = .25 \quad \text{dimensionless} \quad (6-11)$$

$$\alpha = 2 \times 10^{-2} \quad \text{dimensionless} \quad (6-12)$$

and therefore

$$K = .25 + j 2 \times 10^{-2} \quad (6-13)$$

Using the MSG transmission coefficient expression gives

$$T = \frac{2}{1+K} \exp \left(j k_0 h \frac{K-1}{2} \right) \quad (6-14)$$

$$T = \frac{2}{1 + .25 + j 2 \times 10^{-2}} \exp \left(j \frac{2\pi \times 10^{10}}{3 \times 10^2} h \cdot \frac{.25 + j 2 \times 10^{-2} - 1}{2} \right) \quad (6-15)$$

The plasma thickness, h , about a spacecraft [4] is typically taken to be approximately one half the diameter of the spacecraft. Assuming the spacecraft is two meters in diameter a plasma thickness of one meter is present. Then

$$T = \frac{2}{1.25 + j 2 \times 10^{-2}} \exp \left(j \frac{2\pi \times 10^{10}}{3 \times 10^2} \cdot \frac{.75 + j 2 \times 10^{-2}}{2} \right) \quad (6-16)$$

$$|T| = .197 = -7 \text{ db} \quad (6-17)$$

Using the Bremmer approximation

$$T = \kappa^{\frac{1}{2}} \exp \left(j \kappa h \frac{2\kappa^2 - \kappa - 1}{3\kappa + 3} \right)$$

$$T = [.25 + j.02]^{\frac{1}{2}} \exp \left[j \frac{2\pi \times 10^{10}}{3 \times 10^8} \frac{2(.25 + j.02)^2 - .25 - .02j - 1}{3(.25 + j.02) + 3} \right] \quad (6-18)$$

$$|T| = .125 = -6.3 \text{ db} \quad (6-19)$$

The difference between these two approximations is .7 db or about 17 percent.

The effects of plasma propagation loss as a function of frequency have been calculated using the MSG approximation and are plotted in Figure 13. The calculated propagation loss as a function of spacecraft position is shown in Figure 14. Figure 13 depicts the critical region between communication and blackout (10 db to 20 db) for an earth orbital re-entering vehicle at an altitude of 250 kilofeet. The critical portion of the plasma propagation loss versus frequency relationship is shown in Figure 14 for a 10 KMc communication frequency.

Both figures demonstrate that blackout occurs rather abruptly, with respect to both frequency and altitude, as a spacecraft re-enters the earth's atmosphere.

A comparison between the computed results of the invariant imbedding techniques using plasma parameter values specified in this study, and other results is shown in Figure 15. It can be seen from the figure that the invariant imbedding technique predicts Apollo re-entry blackout close to positions of the other predictions and measurements. The invariant imbedding approach appears to be conservative, predicting blackout slightly before (5 to 10 K ft) it actually occurs.

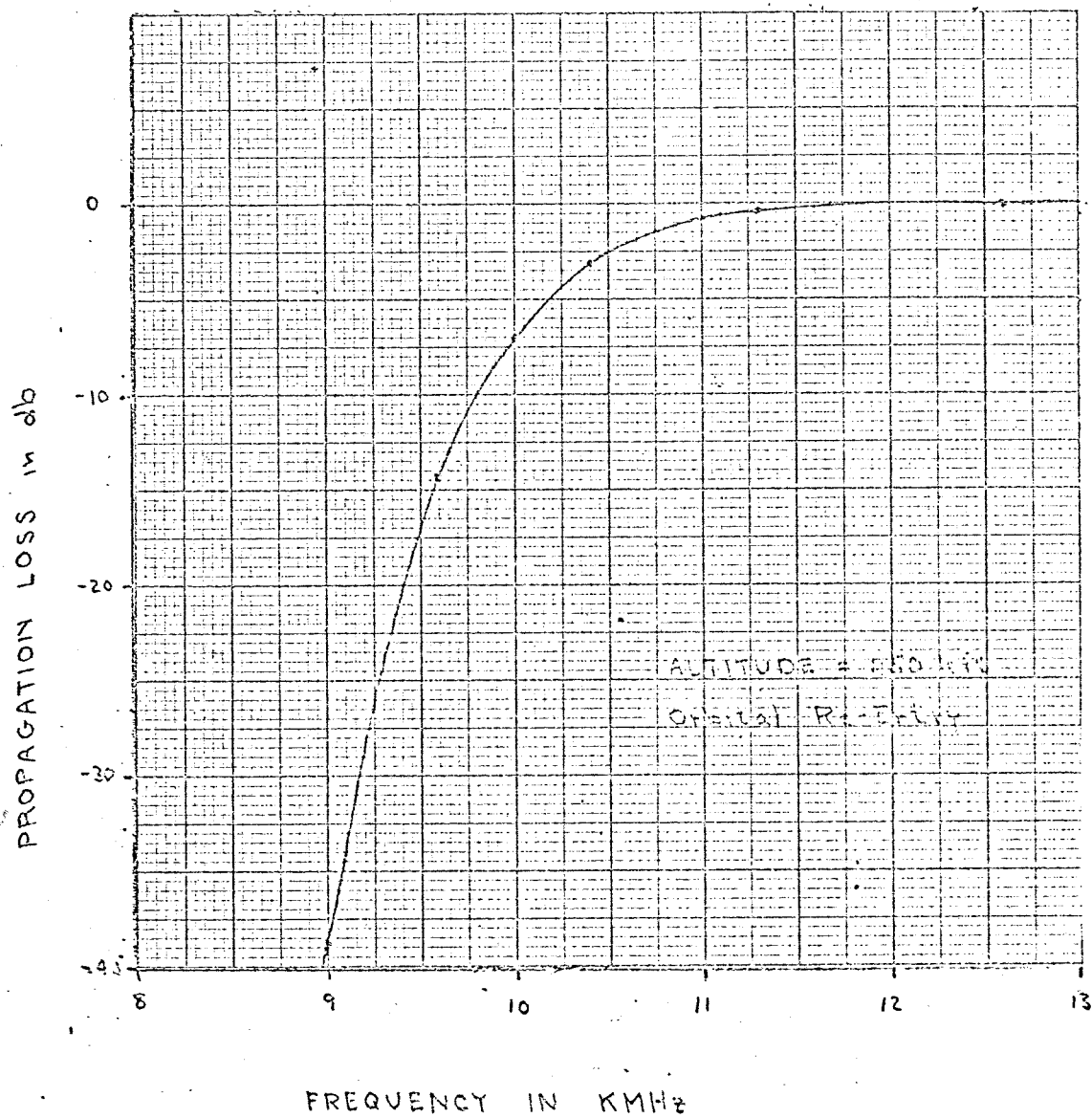


Figure 13. PLASMA PROPAGATION LOSS VERSUS FREQUENCY

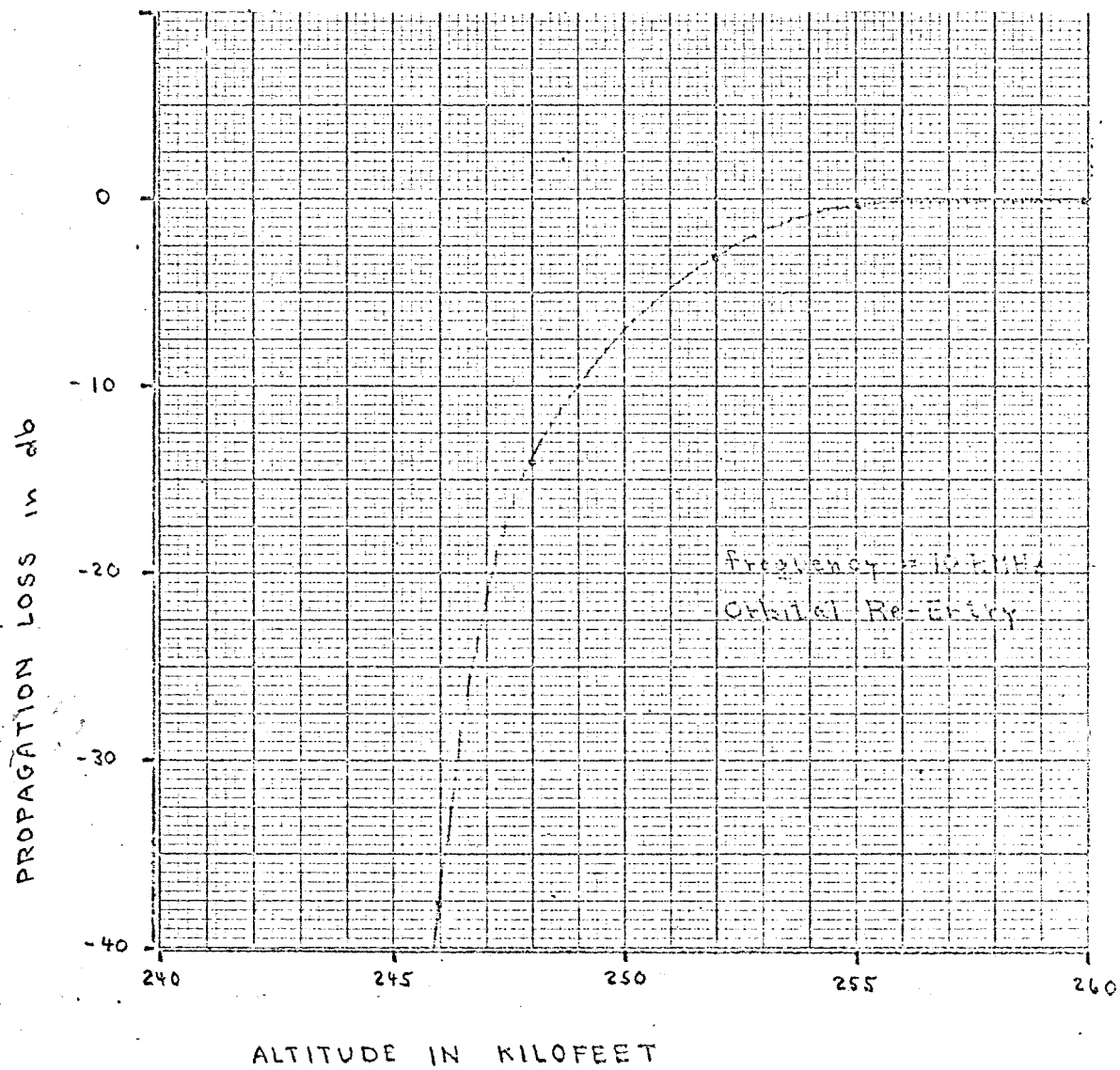
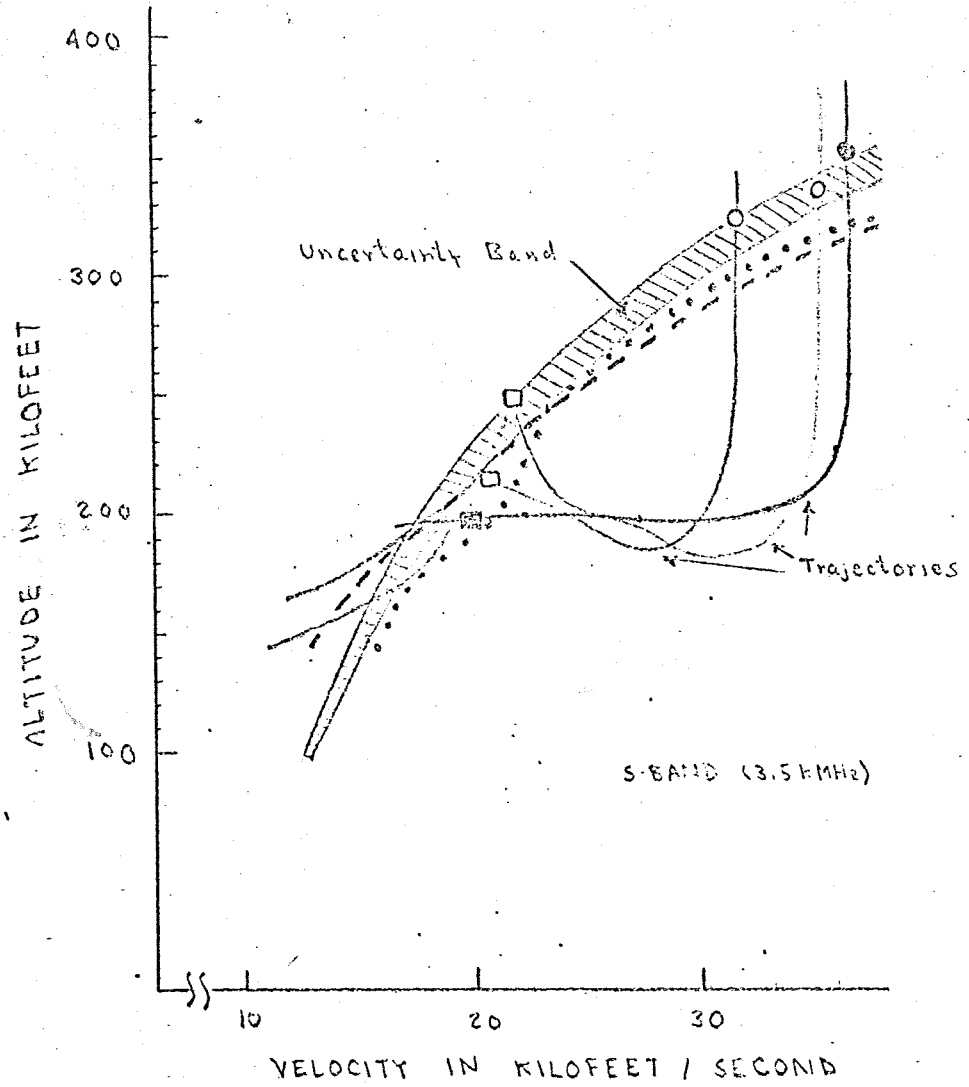


Figure 14. PLASMA PROPAGATION LOSS VERSUS ALTITUDE



Legend

- Cornell Aeronautical Laboratory, State of the art prediction, Nov., 1968 (inviscid flow, pure air)
- Lehnert and Rosenbaum, 1965
- Huber, 1967 (based on ablation product impurity ionization)
- NASA measured blackout and acquisition points
 = acquisition = blackout
- From invariant imbedding technique and data used in this report. = blackout = acquisition

Figure 15. Comparison of Measured and Predicted Blackout Points for Apollo Re-Entry at S-Band

VII. Summary

In this thesis an invariant imbedding technique has been developed to predict propagation losses through an inhomogeneous plasma. The development began by discussing the reasons why and the corresponding conditions under which a plasma is formed. Next, the general nature of plasmas and their descriptive parameters are discussed. Then, the results of an extensive literature survey are presented, providing numerical values to the various plasma parameters that describe typical spacecraft re-entry situations.

At this point, the invariant imbedding computational procedure is developed in terms of the inhomogeneous plasma descriptors. A Riccati type differential equation describing propagation through the plasma results from the application of the invariant imbedding techniques. This type of equation lends itself to computerized solution (being pursued by Professor R. B. Heller at GWU) but two analytical approximations [8] developed elsewhere are used in this study to arrive at solutions.

In the final chapter, the actual plasma parameter values occurring during re-entry situations are used as inputs to the expressions of the previous chapter to predict the magnitude of propagation losses. These losses are computed for several situations and are presented in terms of decibels over free space loss. Finally, the blackout and acquisition points computed from the invariant imbedding technique and data collected in this study are compared with calculated and measured values taken from other sources. The results of the comparison show the values obtained from this study to be in fairly close agreement with the other predictions.

VIII. Bibliography

- [1] M.A. Uman, "Introduction to Plasma Physics," McGraw-Hill Book Company
- [2] R. Bellman, "Perturbation Techniques in Mathematics, Physics, and Engineering," Hold, Rinehart and Winston, Inc., January 1960.
- [3] J.E. Drummond, "Radio Propagation in Re-Entry Plasmas," Boeing Scientific Research Laboratories Document D1-82-0698, October 1967.
- [4] F.H. Mitchell, "Communication System Blackout During Re-Entry of Large Vehicles," Proceedings of the IEEE, Vol. 55, No. 5, May 1967.
- [5] Ramo, Whinnery, and Van Duzer, "Fields and Waves in Communication Electronics," John Wiley & Sons, Inc., New York, 1965.
- [6] E.C. Jordan, "Electromagnetic Waves and Radiating Systems," Prentice-Hall, Inc., Englewood Cliffs, N.J., 1950.
- [7] R. Bellman and R. Kalala, "Functional Equations, Wave Propagation and Invariant Imbedding," Journal of Mathematics and Mechanics, Vol. 8, No. 5, pp. 683-704.
- [8] C.J. MacCallum, "Invariant Imbedding and Wave Propagation in Inhomogeneous Media," SC-4669 (RR), Sandia Corporation, September 1962.
- [9] M.G. Dunn, J.W. Daiber, J.R. Lordi, and R.E. Mates, "Estimates of Nonequilibrium Ionization Phenomena in the Inviscous Apollo Plasma Sheath," NASA CR-596, September 1966.
- [10] D.W. Boyer, "An Investigation of S-Band Signal Transmission Through Apollo Re-Entry Plasma," Cornell Aeronautical Laboratory, Report AI-2187-A-11, January 1969.
- [11] I.P. Shkarofsky, T.W. Johnston, and M.P. Backynski, "Particle Kinetics of Plasmas," Addison-Wesley Publishing Co., 1966.
- [12] R. Lehnert and B. Rosenbaum, "Plasma Effects on Apollo Re-Entry Communications," Goddard Space Flight Center, Rep. X-513-64-8, January 1964.
- [13] R. Hermann, "Hypersonic Aerodynamic Problems at Re-Entry of Space Vehicles," University of Alabama Research Institute, Huntsville, Report 29, November 1965.
- [14] G. Tyras, P.C. Bargelotes, J.M. Hamm, and R.R. Schell, "An Experimental Study of Plasma Effects on Antennas," Radio Science Journal of Research, Vol. 69D, No. 6, June 1965.

- [15] E.J. Baghdady, "Effects of Exhaust Plasmas upon Signal Transmission to and from Rocket Powered Vehicles," Proceedings of the IEEE, Vol. 54, No. 9, September 1966.
- [16] E.A. Grahm, "On the Propagation and Diffraction of Electromagnetic Waves in an Inhomogeneous, Magnetic Medium," Applied Optics, Vol. 4, No. 11, November 1965.
- [17] A.K. Jordan, "The Effects of Electron Collisions on Electric Dipole Radiation Through a Conical Plasma Sheath," IEEE, Transactions on Antennas and Propagation, Vol. AP-16, No. 1, January 1968.

44

Distribution List

NASA/Langley Research Center:

Dr. John E. DuBerg, Associate Director
Mr. P. M. Lovell, Jr., University Affairs Officer
Mr. W. F. Croswell, Antenna Research Section, F.I.D.
Mr. R. L. Trimpi, Head, Reentry Physics Branch, A.P.D.

NASA Headquarters:

Mr. F. B. Smith, Asst. Administrator for University Affairs
Miss Winnie P. Morgan, Code USI (5 copies)

Defense Documentation Center: (5 copies)

George Washington University:

Dean H. Liebowitz, School of Engineering & Applied Science
Dr. Carl Lange, Administrator of Sponsored Research
Dr. John L. Whitesides, Jr., NASA/Langley Research Center
Library

DOCUMENT CONTROL DATA - R & D

(Security classification of title, body of abstract and indexing annotation must be entered when the overall report is classified)

1. ORIGINATING ACTIVITY (Corporate author) School of Engineering & Applied Science The George Washington University		2a. REPORT SECURITY CLASSIFICATION Unclassified	
		2b. GROUP	
3. REPORT TITLE INVARIANT IMBEDDING TECHNIQUE APPLIED TO THE PROPAGATION OF ELECTROMAGNETIC WAVES THROUGH INHOMOGENECUS RE-ENTRY PLASMAS			
4. DESCRIPTIVE NOTES (Type of report and inclusive dates)			
5. AUTHOR(S) (First name, middle initial, last name) Terence G. Ryan Robert B. Heller			
6. REPORT DATE June 7, 1970		7a. TOTAL NO. OF PAGES 48	7b. NO. OF REFS 17
8a. CONTRACT OR GRANT NO. NASA Grant NGR 09-010-053		9a. ORIGINATOR'S REPORT NUMBER(S)	
b. PROJECT NO.			
c.		9b. OTHER REPORT NO(S) (Any other numbers that may be assigned this report)	
d.			
10. DISTRIBUTION STATEMENT Distribution of this document is unlimited.			
11. SUPPLEMENTARY NOTES		12. SPONSORING MILITARY ACTIVITY	
13. ABSTRACT <p>The problem of communicating through a re-entry plasma arose out of a study being done by the George Washington University School of Engineering and Applied Science under the direction of Professor R. B. Heller for the National Aeronautics and Space Administration, Langley, Virginia. Propagation through re-entry plasmas, the topic of this study, is intended to serve as a contribution toward this effort. Lengthy computerized computational procedures have been utilized in the past to solve the inhomogeneous second order wave equation and thus predict propagation losses in an inhomogeneous media. This study presents a technique yielding approximate solutions that may be calculated without the use of a computer or lengthy computational procedures. Accuracies to within a few percent of those due to lengthy computer runs are obtained.</p> <p>The re-entry communications problem is a serious one resulting in complete communication blackout during critical phases of space missions. It is the purpose of this study to develop, via an invariant imbedding technique, a means of predicting signal losses through an inhomogeneous re-entry plasma.</p>			

14. KEY WORDS	LINK A		LINK B		LINK C	
	ROLE	WT	ROLE	WT	ROLE	WT

THE GEORGE WASHINGTON UNIVERSITY

BENEATH THIS PLAQUE
IS BURIED
A VAULT FOR THE FUTURE
IN THE YEAR 2056

THE STORY OF ENGINEERING IN THIS YEAR OF THE PLACING OF THE VAULT AND
ENGINEERING HOPES FOR THE TOMORROWS AS WRITTEN IN THE RECORDS OF THE
FOLLOWING GOVERNMENTAL AND PROFESSIONAL ENGINEERING ORGANIZATIONS AND
THOSE OF THIS GEORGE WASHINGTON UNIVERSITY.

BOARD OF COMMISSIONERS, DISTRICT OF COLUMBIA
UNITED STATES ATOMIC ENERGY COMMISSION
DEPARTMENT OF THE ARMY, UNITED STATES OF AMERICA
DEPARTMENT OF THE NAVY, UNITED STATES OF AMERICA
DEPARTMENT OF THE AIR FORCE, UNITED STATES OF AMERICA
NATIONAL ADVISORY COMMITTEE FOR AERONAUTICS
NATIONAL BUREAU OF STANDARDS, U.S. DEPARTMENT OF COMMERCE
AMERICAN SOCIETY OF CIVIL ENGINEERS
AMERICAN INSTITUTE OF ELECTRICAL ENGINEERS
THE AMERICAN SOCIETY OF MECHANICAL ENGINEERS
THE SOCIETY OF AMERICAN MILITARY ENGINEERS
AMERICAN INSTITUTE OF MINING & METALLURGICAL ENGINEERS
DISTRICT OF COLUMBIA SOCIETY OF PROFESSIONAL ENGINEERS, INC.
THE INSTITUTE OF RADIO ENGINEERS, INC.
THE CHEMICAL ENGINEERS CLUB OF WASHINGTON
WASHINGTON SOCIETY OF ENGINEERS
FAULKNER KINGSBURY & STENHOUSE - ARCHITECTS
CHARLES H. TOMPKINS COMPANY - BUILDERS
SOCIETY OF WOMEN ENGINEERS
NATIONAL ACADEMY OF SCIENCES, NATIONAL RESEARCH COUNCIL

THE PURPOSE OF THIS VAULT IS INSPIRED BY AND IS DEDICATED TO
CHARLES HOOK TOMPKINS, DOCTOR OF ENGINEERING
BECAUSE OF HIS ENGINEERING CONTRIBUTIONS TO THIS UNIVERSITY, TO HIS
COMMUNITY, TO HIS NATION, AND TO OTHER NATIONS.

BY THE GEORGE WASHINGTON UNIVERSITY.

ROBERT V. FLEMING
CHAIRMAN OF THE BOARD OF TRUSTEES

CLOYD H. MARVIN
PRESIDENT

JUNE THE TWENTIETH
1955

To cope with the expanding technology, our society must be assured of a continuing supply of rigorously trained and educated engineers. The School of Engineering and Applied Science is completely committed to this objective.